An analytical model for cable bolts considering crack propagation in grout

Danqi Li
WA School of Mines, Curtin University, Kalgoorlie, WA, Australia

ABSTRACT: Understanding the mechanical behaviour of cable bolts under axial loading from analytical perspective is essential and economic for selecting the most appropriate cable bolt for a specific scenario and also the ground support system design. This study develops a novel analytical model coupling the crack propagation in the grout annulus to capture the load-displacement performance of cable bolts under axial loading. The majority of the input parameters associated with mechanic properties of the cable bolt and grout are readily determinable by laboratory tests. At the end, the capability of the proposed model to simulate the performance of cable bolts under axial loading is demonstrated by validating against experimental results in the literature.

Keywords: Analytical model, Cable bolts, Pull out test; Crack propagation

1 INTRODUCTION

The grouted cable bolt and rock bolt are effective and efficient to the roof support in underground excavations given that they can restrict the movement of the excavation roof by transferring the dead weight of the disturbed rockmass close to the excavation into the competent rockmass far into the country rock (Li et al., 2018a; Li et al., 2018b). To date, there has been limited analytical research on the load-displacement performance of cable bolts under axial loading. The works can be categorised into two different approaches. One is associated with various solutions to the force equilibrium equation for the micro element of the grouted cable bolt (Li and Stillborg, 1999; Ma et al., 2014; Ren et al., 2010; Yuan et al., 2004). The common limitation of such pure mathematical methods is that all the input parameters are determined by back analysis and lack of physical meanings associated with rock mechanics. The other one is developed based on the modified Mohr-Coulomb failure mechanism at the cable bolt to grout interface coupling the load transfer in the grout annulus from the confinement outside the grout (Li et al., 2021a; Li et al., 2021b; Li et al., 2019; Li et al., 2017). The limitation of such models is the over simplistic assumption that the crack in the grout annulus remains fully opened over the full displacement of the cable bolt during pull-out test leading to the constant confinement environment throughout the test. However, in reality, the grouted cable bolt is under an ongoing change of the confinement over the displacement of the cable bolt.

In this study, a novel analytical model is proposed to simulate the load-displacement performance of cable bolts under axial loading subjected to the ongoing varying confining pressure on the grouted cable bolt resulted from crack propagation. The formation of such cracks will undergo three phases being crack initiation, crack propagation and crack fully split in sequence leading to different load transfer mechanisms in the grout annulus during the full displacement of the cable bolt. The boundaries between different phases were also determined in order to develop smooth transitions between different stages in the load-displacement behaviour of cable bolts. The analytical results are calibrated and validated against a number of pull-out test results obtained from literature to demonstrate its capability to capture the behaviour of cable bolts under axial loading.

2 RADIAL CRACK INITIATION AND PROPAGATION

2.1 Load transfer in grout annulus

Considering the significant dilation resulted from the bulge structure during the pull-out test, it is assumed that the expansion of the cylindrical grout or even split will occur under plane strain conditions. In addition, the longitudinal stress on the grout annulus will not be considered in this study given its marginal or even negligible axial movement during the test. As a result, for the radially symmetric case with no body force, the differential equation of force equilibrium proposed by Ladanyi (1967) can be used :

$$\frac{d\sigma_r}{dr} + \frac{\sigma_r - \sigma_t}{r} = 0 \tag{1}$$

where σ_r is the stress in the radial direction that can result in expansion or confinement, σ_t is the tangential tensile stress that can result in the radial crack in the grout annulus. Such a differential equation is able to capture the progressive change of both radial stress and tangential tensile stress in grout annulus at different radius. Considering the grouted cable bolt has two interfaces including cable bolt to grout interface and external circumference of the grout to confinement interface, the difference between the confining pressures at the two interfaces should be considered due to the load transfer in the grout annulus. Therefore, one possible solution to Eq. 1 can be in the following form:

$$\sigma_r = \frac{p_1 r_1^2 - p_2 r_2^2}{r_2^2 - r_1^2} - \frac{(p_1 - p_2) r_1^2 r_2^2}{r_2^2 - r_1^2} \frac{1}{r^2} \tag{2}$$

$$\sigma_t = \frac{p_1 r_1^2 - p_2 r_2^2}{r_2^2 - r_1^2} + \frac{(p_1 - p_2) r_1^2 r_2^2}{r_2^2 - r_1^2} \frac{1}{r^2} \tag{3}$$

$$u_r = \frac{(1+\mu)(1-2\mu)}{E} \frac{p_1 r_1^2 - p_2 r_2^2}{r_2^2 - r_1^2} r + \frac{(1+\mu)}{E} \frac{(p_1 - p_2) r_1^2 r_2^2}{r_2^2 - r_1^2} \frac{1}{r} \tag{4}$$

where p_1 is the confining pressure at the cable bolt to grout interface, p_2 is the confining pressure at the external circumference of the cylindrical grout, r_1 is the radius of the internal circumference of the grout, r_2 is the radius of the external circumference of the grout, r is the radius between r_1 and r_2, μ is the poison ratio of the grout, E is the Young's Modulus of grout and u_r is the radial displacement at radius of r. In addition, two governing equations for axial load and dilation at the cable bolt to grout interface were obtained by Li et al. (2017) according to:

$$F_p = A p_1 tan(i_{mob} + \varphi) \tag{5}$$

$$u_{r1} = \tan(\frac{e^{-Cu_a}}{2 - e^{-Cu_a}} i_0) e^{\frac{-p_1}{UCS}} u_a \tag{6}$$

where F_p is the peak axial load, p_1 is the confining pressure at the interface between the bolt and grout, φ is the basic friction angle of the grout, i_{mob} is the mobilised asperity angle and A is the surface area of the front section of the bulge, C was also provided in the work by Li et al. (2017) (see in Figure 1).

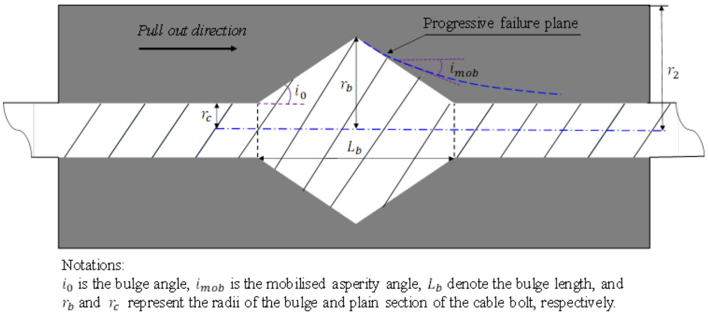

Figure 1. Illustration of the progressive failure plane during pull-out test of cable bolts.

2.2 *Crack initiation*

At the beginning of the pull-out test of cable bolts, there is no relative slip between the cable bolt and grout until reaching a threshold point that the cable bolt will start to slip and hence dilation will occur. Such a dilation will lead to an increase in the confining pressure at the cable bolt to grout interface and tangential tensile stress in the grout annulus. As a result, the crack will initiate when the induced tangential tensile stress at the internal circumference of the grout annulus exceeds the tensile strength of the grout (T_s) (see in Figure 2).

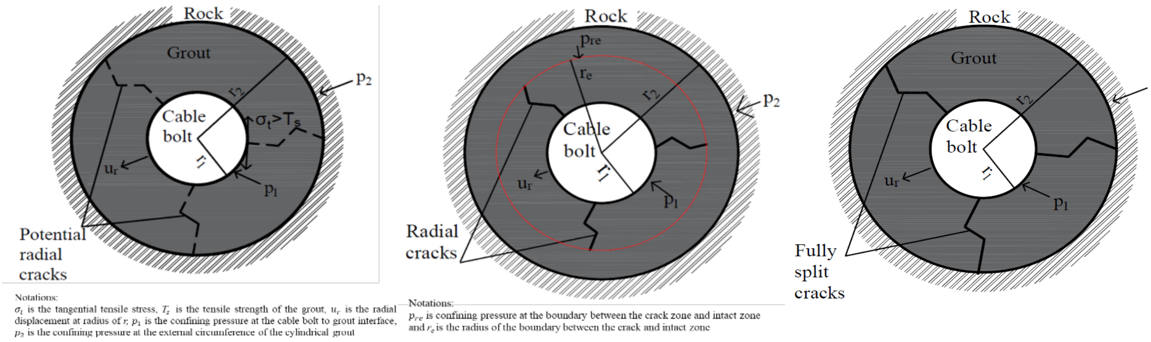

Figure 2. Crack initiation and propagation.

The confining pressure at the cable bolt to grout interface before the cable bolt starts to slip can be obtained by rearranging the Eq. 4 and setting u_r equals zero:

$$p_1 = \frac{2(1-\mu) r_2^2 p_2}{(1-2\mu) r_1^2 + r_2^2} \tag{7}$$

Once the slip occurs but before the initiation of the radial crack, the relationship between p_1 and dilation u can be derived based on Eq. (4):

$$p_1 = \frac{E(r_2^2 - r_1^2)u_r}{(1+\mu)r_1((1-2\mu)r_1^2 + r_2^2)} + \frac{2(1-\mu)r_2^2 p_2}{(1-2\mu)r_1^2 + r_2^2} \tag{8}$$

The partial differential form of p_1 with respect to dilation u_r is:

$$\frac{\partial p_1}{\partial u_r} = \frac{E(r_2^2 - r_1^2)}{(1+\mu)r_1((1-2\mu)r_1^2 + r_2^2)} \tag{9}$$

Also, the partial differential form of the dilation u_r with respect to axial displacement u_a can be obtained from Eq. 5 according to:

$$\frac{\partial u_r}{\partial u_a} = \tan(i_{mob})e^{\frac{-p_1}{UCS}} + u_a\big(\mathrm{sectan}(i_{mob})\big)^2 e^{\frac{-p_1}{UCS}}\Big(\frac{-2Ci_{mob}}{2 - e^{-Cu_a}} + \frac{2u_a K_c i_{mob}}{(2 - e^{-Cu_a})L_b(r_b - r_c)}\Big) \tag{10}$$

As a result, the differential increment of the confining pressure at cable bolt to grout interface (p_1) over incremental increase in axial displacement (u_a) can be determined by combining Eqs. 9 and 10:

$$\frac{\partial p_1}{\partial u_a} = \frac{E(r_2^2 - r_1^2)}{(1+\mu)r_1\big((1-2\mu)r_1^2 + r_2^2\big)}\Big(\tan(i_{mob})e^{\frac{-p_1}{UCS}} + u_a\big(\mathrm{sectan}(i_{mob})\big)^2 e^{\frac{-p_1}{UCS}}\Big(\frac{-2Ci_{mob}}{2 - e^{-Cu_a}} + \frac{2u_a K_c i_{mob}}{(2 - e^{-Cu_a})L_b(r_b - r_c)}\Big)\Big) \tag{11}$$

In addition, the incremental change in the axial load of the cable bolt over the incremental increase in the axial displacement can be derived from the Eq. 5:

$$\frac{\partial F_p}{\partial u_a} = A\tan(i_{mob} + \phi)\cdot\frac{\partial p_1}{\partial u_a} + p_1\big(\mathrm{sectan}(i_{mob} + \phi)\big)^2\cdot\Big(\frac{-2Ci_{mob}}{2 - e^{-Cu_a}} + \frac{2u_a K_c i_{mob}}{(2 - e^{-Cu_a})L_b(r_b - r_c)}\Big) \tag{12}$$

and, $\frac{\partial p_1}{\partial u_a}$ has been defined in Eqs. 11.

Therefore, the load-displacement behaviour of the cable bolt under axial loading before the crack initiation is governed by Eqs. 11 and 12 until reaching a point where the tangential tensile stress at the internal circumference of the grout annulus (σ_t) exceeds the tensile strength of the grout (Ts) according to:

$$\sigma_t = T_s = \frac{p_1 r_1^2 - p_2 r_2^2}{r_2^2 - r_1^2} + \frac{(p_1 - p_2)r_1^2 r_2^2}{r_2^2 - r_1^2}\frac{1}{r_1^2} \tag{13}$$

Rearrangement of Eq. 13 yields:

$$p_1^t = \frac{T_s(r_2^2 - r_1^2) + 2p_2 r_2^2}{r_1^2 + r_2^2} \tag{14}$$

where p_1^t is the induced confining pressure at the internal circumference of the grout annulus that leads to the crack initiation. Once the confining pressure at the cable bolt to grout interface (p_1) exceeds p_1^t, the failure in the grout annulus will enter the second phase being the crack propagation phase.

2.3 *Crack propagation*

During the crack propagation of the grout annulus, partial split cracks are developed leading to the formation of two regions being the crack zone as well as the intact zone outside the crack zone (Fig. 3). It is assumed the grout annulus is homogeneous and the rates of the radial crack propagation along different directions are same. Therefore, the crack zone has a uniform radius of r_e and confining pressure (p_{re}) at the boundary between the crack zone and intact zone regardless of the propagation directions.

Replacing p_1 and r_1 in Eq. 14 with p_{re} and re, and rearranging the results equation leads to:

$$p_{re} = \frac{T_s(r_2^2 - r_e^2) + 2p_2 r_2^2}{r_e^2 + r_2^2} \quad (15)$$

For the crack zone, the relationship between p_{re} and p_1 will follow the equation proposed by Hyett et al. (1995) according to:

$$p_1 = p_{re}\frac{r_e}{r_1} \quad (16)$$

In addition, it is proposed first time ever that the rate of the radial crack propagation will follow the logarithm function according to:

$$r_e = ln\, u_a \qquad \text{for} \qquad r_1 \le r_e \le r_2 \quad (17)$$

As a result, the incremental change of the confining pressure p_1 at the cable bolt to grout interface due to the unit increase in axial displacement can be obtained by coupling Eqs. 15 and 16 to 17:

$$\frac{\partial p_1}{\partial u_a} = \frac{\partial p_1}{\partial p_{re}}\frac{\partial p_{re}}{\partial r_e}\frac{\partial r_e}{\partial u_a} + \frac{\partial p_1}{\partial r_e}\frac{\partial r_e}{\partial u_a} = \frac{1}{u_a}\left(\frac{-4r_e^2 r_2^2(T_s + p_2)}{r_1(r_e^2 + r_2^2)^2} + \frac{p_{re}}{r}\right) \quad (18)$$

Therefore, Eq. 18 can be substituted into Eq. 12 to capture the incremental change in the axial load of the cable bolt against axial displacement.

3 MODEL VALIDATION

Moosavi (1997) tested the Garfold Bulbed cable bolt and the Nutcase cable bolt under constant confining pressure using a modified Hoek Cell. The confining pressure varied from 2 to 15 MPa. All the input parameters are listed in Table 1. The model simulations of the load-displacement performance of the Garford Bulbed and the Nutcase cable bolts over the axial displacement of 50 mm are presented in Figure 3, respectively. Both figures confirm that there is a good agreement between the model simulations and the experimental results at different confining pressures.

Table 1. Model input parameters.

Cable bolt	r_1 (mm)	r_2 (mm)	H_b (mm)	L_b (mm)	r_c (mm)	r_b (mm)	i_0 (°)	E (GPa)	μ	UCS (MPa)	φ
Nutcase	7.6	31.75	150	100	7.6	10.5	3.3	18.6	0.2	50	21
Garford Bulbed	7.6	31.75	150	100	7.6	12.5	5.5	18.6	0.2	50	21

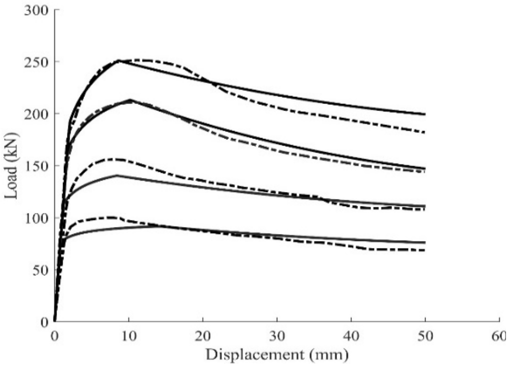

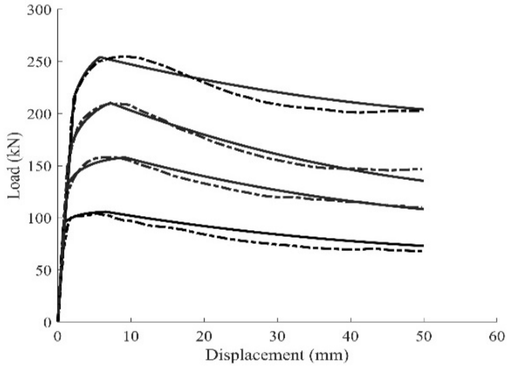

Figure 3. Model validation: a) Garford bulbed cable bolt (left) and b) Nutcase cable bolt (right), Solid lines are simulations and dash line are experimental results.

4 CONCLUSIONS

An analytical model was developed for simulating the full load-displacement performance of the cable bolt under axial loading subjected to varying confining pressures due to the crack propagation in the grout annulus. The proposed analytical model in this study was calibrated with the experimental data of the Garfold Bulbed and the Nutcase cable bolts. The close agreement between the model simulations and the experimental results confirms the validity of the proposed constitutive model.

REFERENCES

Hyett, A.J., Bawden, W.F., Macsporran, G.R., Moosavi, M., 1995. A constituitive law for bond failure of fully grouted cable bolts using a modified hoek cell. International Journal for Numerical and Analytical Methods in Geomechanics 32, 11-36.

Ladanyi, B., 1967. Expansion of cavities in brittle media. International Journal of Rock Mechanics and Mining Sciences & Geomechanics Abstracts 4, 301-328.

Li, C., Stillborg, B., 1999. Analytical models for rock bolts. International Journal of Rock Mechanics and Mining Sciences 36, 1013-1029.

Li, D., Cai, M., Masoumi, H., 2021a. A constitutive model for modified cable bolts exhibiting cone shaped failure mode. International Journal of Rock Mechanics and Mining Sciences 145, 104855.

Li, D., Li, Y., Chen, J., Masoumi, H., 2021b. An analytical model for axial performance of rock bolts under constant confining pressure based on continuously yielding criterion. Tunnelling and Underground Space Technology 113, 103955.

Li, D., Masoumi, H., Hagan, P.C., Saydam, S., 2019. Experimental and analytical study on the mechanical behaviour of cable bolts subjected to axial loading and constant normal stiffness. International Journal of Rock Mechanics and Mining Sciences 113, 83-91.

Li, D., Masoumi, H., Saydam, S., Hagan, P.C., 2017. A constitutive model for load-displacement performance of modified cable bolts. Tunnelling and Underground Space Technology 68, 95-105.

Li, D., Masoumi, H., Saydam, S., Hagan, P.C., 2018a. Mechanical characterisation of modified cable bolts under axial loading: An extensive parametric study. Rock Mechanics and Rock Engineering 51, 2895-2910.

Li, D., Masoumi, H., Saydam, S., Hagan, P.C., Asadizadeh, M., 2018b. Parametric study of fully grouted cable bolts subjected to axial loading. Canadian Geotechnical Journal 56, 1514-1525.

Ma, S., Nemcik, J., Aziz, N., Zhang, Z., 2014. Analytical model for rock bolts reaching free end slip. Construction and Building Materials 57, 30-37.

Moosavi, M., 1997. Load distribution along fully groutedd cable bolts based on constituitive models obtained from modified Hoek cells, Department of Mining Engineering. Queen's University, Kingston.

Ren, F.F., Yang, Z.J., Chen, J.F., Chen, W.W., 2010. An analytical analysis of the full-range behaviour of grouted rockbolts based on a tri-linear bond-slip model. Construction and Building Materials 24, 361-370.

Yuan, H., Teng, J.G., Seracino, R., Wu, Z.S., Yao, J., 2004. Full-range behavior of FRP-to-concrete bonded joints. Engineering Structures 26, 553-565.